Planetary and Space Science 66 (2012) 165–172

Contents lists available at SciVerse ScienceDirect

Planetary and Space Science

journal homepage: www.elsevier.com/locate/pss

The Rosetta campaign to detect an exosphere at Lutetia

A.D. Morse[a,*], K. Altwegg[b], D.J. Andrews[a], H.U. Auster[c], C.M. Carr[d], M. Galand[d], F. Goesmann[e], S. Gulkis[f], S. Lee[f], I. Richter[c], S. Sheridan[a], S.A. Stern[g], M.F. A'Hearn[h], P. Feldman[i], J. Parker[j], K.D. Retherford[j], H.A. Weaver[k], I.P. Wright[a]

[a] *Planetary and Space Sciences Research Institute, The Open University, Walton Hall, Milton Keynes MK7 6AA, England, UK*
[b] *Physikalisches Institut, Universität Bern, Sidlerstr. 5, 3012 Bern, Switzerland*
[c] *Institut für Geophysik und Extraterrestrische Physik der Technischen Universität Braunschweig, Mendelssohnstrasse 3, 38106 Braunschweig, Germany*
[d] *The Blackett Laboratory, Imperial College, London SW7 2BW, UK*
[e] *Max Planck Institute for Solar System Research, Katlenburg-Lindau, Germany*
[f] *Jet Propulsion Laboratory, California Institute of Technology, 4800 Oak Grove Drive, MS 169-506 Pasadena, CA 91109, USA*
[g] *National Aeronautics and Space Administration, Washington, DC, USA*
[h] *Department of Astronomy, University of Maryland, College Park, MD 20742 2421, USA*
[i] *Johns Hopkins University, Baltimore, MD 21218 2695, USA*
[j] *Southwest Research Institute, 1050 Walnut Street, Suite 300, Boulder, CO 80302, USA*
[k] *Applied Physics Laboratory, Laurel, MD 20723, USA*

ARTICLE INFO

Article history:
Received 25 July 2011
Received in revised form
5 January 2012
Accepted 6 January 2012
Available online 25 January 2012

Keywords:
Rosetta
Lutetia
Exosphere
Asteroid
Comet

ABSTRACT

On 10th July 2010 the Rosetta spacecraft passed within 3160 km of asteroid 21 Lutetia during which seven instruments attempted to detect an exosphere. A comparison of the sensitivity is made between the different instruments based on a simple spherical out-gassing point source model, which was used to infer that the Lutetia exosphere production rate was determined by MIRO to be $<4.3\times10^{23}$ molecules s^{-1} for water and by ROSINA RTOF to be $<1.7\times10^{25}$ molecules s^{-1} for carbon monoxide. Consideration of the flyby geometry and combined instrument operations places further constraints on the exosphere structure and gas production rate. Experience gained during the flyby will prove invaluable for operations planning during Rosetta's approach and orbit of comet 67P/Churyumov–Gerasimenko in 2014.

1. Introduction

Asteroids and comets have traditionally been considered as two separate and distinct classes of minor bodies: the asteroids, mostly residing within the main belt (2.0–3.2 AU), being volatile-depleted and showing no insolation-related activity, and the comets, volatile-rich bodies showing the effects of their transient proximity to the Sun often resulting in the generation of stunning sublimation-driven comae and tails. However, the traditional view of a clear distinction between comets and asteroids has become blurred, starting with the discovery of a coma around asteroid 7968 Elst-Pizarro (Hsieh et al., 2004). Subsequent observations have shown that this body exhibits comet-like behaviour, with periodic out-gassing during perihelion leading to the dual classification 113P/Elst-Pizarro (Hsieh et al., 2010). Further searches have found other asteroids showing out-gassing, leading to their classification as Main Belt Comets (Hsieh and Jewitt, 2006), with their activity attributed to collisions exposing buried volatiles. Evidence for the spectacular results of impacts in the main belt was obtained for a body discovered in 2010 (P/2010 A2). Although originally classified as a comet, on account of it having a tail, it looks increasingly likely that it is, in fact, an asteroid, the tail being the consequence of the recent impact (Jewitt et al., 2010; Snodgrass et al., 2010).

Near-infrared observations indicate that many asteroids (including Lutetia) exhibit adsorption features in the 3 μm region indicative of hydrated mineral (Rivkin et al., 1995, 2000). Further evidence that asteroids are not volatile-poor bodies has been provided by near-infrared observations of 24 Themis (Campins et al., 2010; Rivkin and Emery, 2010) and 65 Cybele (Landsman et al., 2010). The 3.1 μm feature is consistent with water ice being widespread over the surface of the asteroid. Other features in the spectra were best explained by the presence of organics rather than hydrated minerals. In this case, out-gassed species would be expected to have a similar composition to cometary comae. In addition, theoretical modelling (Schorghofer, 2008) has shown

* Corresponding author. Tel.: +44 1908 659509.
E-mail address: A.D.Morse@open.ac.uk (A.D. Morse).

0032-0633/$ - see front matter © 2012 Elsevier Ltd. All rights reserved.
doi:10.1016/j.pss.2012.01.003

that water ice can exist buried within the top few metres of an asteroid over the lifetime of the Solar System. Ice could then be exposed either by impact events or by micrometeorite impact gardening, similar to those on the Moon.

With so much emerging ambiguity about the exact nature of the minor bodies of the Solar System and their relationships, the Rosetta flyby of Lutetia in July 2010 seemed to offer an excellent opportunity to search for evidence of an asteroidal exosphere (especially since Lutetia is a relatively large asteroid). Prior to the encounter, modelling of Lutetia as a volatile-poor, "airless" body, like Mercury or the Moon, indicated that any exosphere would consist mostly of thermally released solar wind species, giving particle densities at the flyby distance (approximately 3000 km) of about $10^5\,m^{-3}$ for hydrogen, $10^4\,m^{-3}$ for helium and a molecular density of $10^2\,m^{-3}$ for H_2O (Schläppi et al., 2008). Other processes, such as solar wind ion sputtering and photon stimulated desorption, were thought likely to impart, respectively, refractory elements and sodium at levels of $\sim 10^3\,m^{-3}$ in each case. So these represented a baseline view of what might be detectable. But this was against the backdrop of a rather traditional view of asteroids and there was in any case another intriguing uncertainty involving the spectral type of the body, which had been rather ambiguously assigned as either M- or C-type. An M-type (metallic) asteroid would be expected to show little out-gassing. However a C-type (carbonaceous) could have much larger out-gassing from water in hydrated minerals and buried ice. Furthermore the oblique spin axis determined by observations prior to the Rosetta encounter (Carry et al., 2010) meant that parts of the asteroid could experience larger solar heating at the sunward facing pole than normally expected.

The Rosetta spacecraft is designed to measure the physical and chemical compositions of comet 67P/Churyumov–Gerasimenko and its coma as it travels towards perihelion. Two of the main science themes are determining physical properties and chemical composition of the coma (e.g. Wirth et al., 2009). As a result, many of the instruments are designed to operate within and measure the relatively high pressure of the coma. However, from the outset, another science goal of the Rosetta mission was to carry out observations during the flyby of two separate asteroids (Glassmeier et al., 2007, 2009a). Within this theme was an opportunity to study the asteroid environment during the flyby. Although any exosphere was expected to be of very low density there are several reasons why this might be enhanced:

(i) water could be preserved for Solar System time-scales if Lutetia was a C-type asteroid as ice buried beneath the surface;
(ii) for the number of months preceeding the encounter the North polar axis of Lutetia was pointing towards the Sun, providing enhanced insolation of the pole;
(iii) a recent impact event might have the capacity to cause out-gassing over a time-scale of thousands of years;
(iv) on the basis of recent observations/modelling there should no longer be any a priori reason to expect an asteroidal exosphere to conform to the notion of some kind of homogenous, spherical shell of material;
(v) Asteroidal out-gassing phenomena may include directional jets.

In addition to the scientific return, the flyby manoeuvre was an opportunity to rehearse co-ordinated instrument activities similar to those that are expected to be carried out at the comet. The various instrument requests and incompatibilities were co-ordinated into the pre-planned timeline. During the flyby the one-way light time of 20 min was similar to that expected at comet encounter, and so all sequences were operated autonomously.

2. Rosetta exosphere campaign

The Rosetta spacecraft has 7 instruments capable of detecting an exosphere: three mass spectrometers, ROSINA (on the Orbiter), Ptolemy and COSAC (both on the Philae Lander); a suite of plasma instruments, RPC (on the Orbiter) and ROMAP (on Philae); and two instruments on the Orbiter, namely Alice, an ultraviolet imaging spectrometer, and MIRO, a microwave instrument. In principle, it would have been highly desirable to have had all of the requisite instruments operating continuously during the flyby. Indeed, during the flyby, as opposed to on-comet investigations, there would have been adequate power resources to allow this. But, nevertheless there were issues. Firstly, the overriding criterion for success during this part of the mission was that the spacecraft flyby at a distance of 3160 km, allowing accurate tracking of the asteroid during Close Approach for imaging reasons (Barucci and Fulchignoni, 2009). Secondly, most instruments desired to be pointing towards the asteroid. Furthermore, it was already known that operation of certain instruments caused interferences for others, so a schedule had to be devised that took account of this. Of particular concern was the effect of interference from the Lander instruments on the RPC instruments because of a current loop between the Lander umbilical and the spacecraft. This can be compensated by simultaneous measurements by ROMAP on the Lander as long as currents used by Lander instruments are well characterised and are constant. However both Ptolemy and COSAC mass spectrometers have high frequency power fluctuations during measurements. Since RPC measurements were considered to be more critical during the flyby it was decided to ensure that Lander current use was constant at least for 12 min on either side of Close Approach (CA).

ROSINA measurements during the Steins flyby (Jäckel et al., 2009) and subsequent analysis of spacecraft out-gassing (Schläppi et al., 2010) indicate that the limit of detection for ROSINA was the spacecraft out-gassing and not the instrument sensitivity. Tests performed earlier during the Cruise Phase had shown that ROSINA could detect an increase in pressure when instruments were switched on and with changes of spacecraft orientation with respect to the Sun. These out-gassing events had a duration of about 1 h. An ideal encounter scenario for the mass spectrometer instruments was to have all other instruments switched off and no changes in spacecraft orientation for about 2 h on either side of CA, clearly incompatible with remote sensing instrument requests to be operating and pointing towards Lutetia. Instrument effects were minimised by having all instruments switched on for at least 4 h before CA so that their effects were at a minimum and constant. Instrument operations during the Lutetia flyby are shown in Fig. 1.

Spacecraft out-gassing was minimised by suitable planning and operation of the spacecraft during the flyby (i.e. CA $\pm$ 4 h). The autonomous use of reaction thrusters, a known source of contamination (Graf et al., 2008), was disabled over a month before Lutetia encounter, spacecraft orientation being achieved by the reaction wheels. The final use of the reaction thrusters was a manual offloading of the reaction wheels at about CA $-$ 36 h. A schematic diagram of the spacecraft is shown in Fig. 2, with most instruments mounted on the $+Z$ panel. For the flyby the spacecraft was orientated so that the $+Z$-axis always pointed towards the asteroid and the Y-axis was perpendicular to the solar illumination with tracking of the asteroid achieved by rotation through the Y-axis as shown in Fig. 3. In this way the $\pm Y$-panels of the spacecraft were not illuminated throughout the flyby. Up to

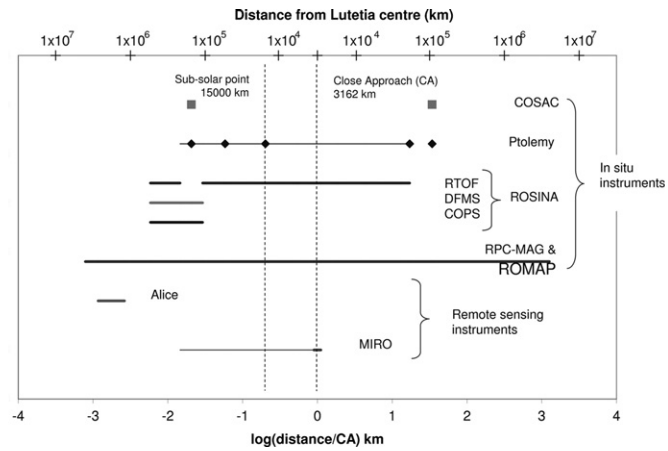

Fig. 1. Instrument operations during the Lutetia flyby, plotted with distance from the asteroid centre. The scale is log of the spacecraft distance to the Closest Approach distance (CA), approximate distance shown on the upper axis. Instruments that were powered on but not making measurements to detect an exosphere are indicated by narrow lines. The mass spectrometer instruments operated during the CA period with only RTOF operating continuously. The RPC and ROMAP instruments operated continuously for 3 days on either side of the encounter. Alice observations were from long distance to gain an overall production rate measurement. MIRO was able to search for a water signal after the sub-solar point at a distance of less than 5000 km to CA.

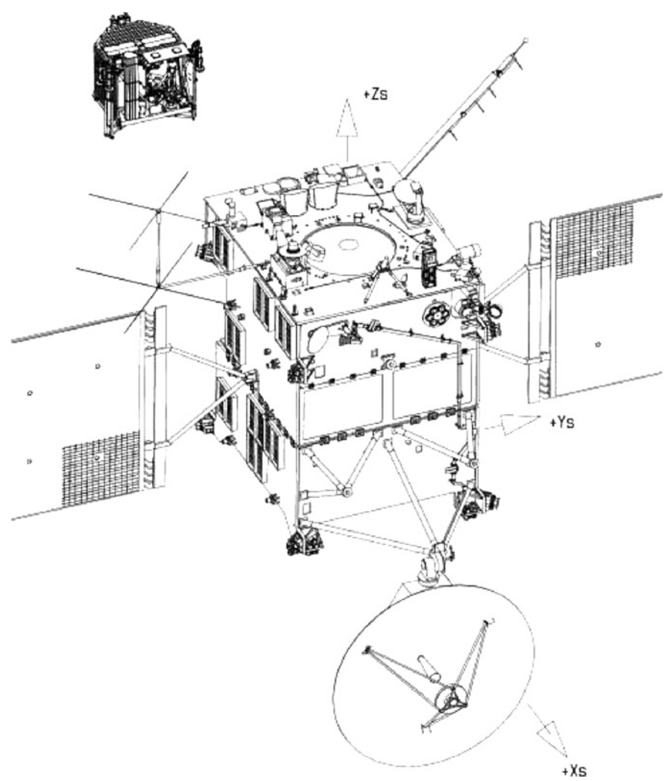

Fig. 2. Schematic diagram of the Rosetta spacecraft (adapted from Accomazzo et al., 2010). Most instruments are on the $+Z$-panel and were pointing towards Lutetia during the flyby. The Lander is attached to the $-X$-panel with Ptolemy Vent pipe pointing towards Lutetia and COSAC vent pipe pointing away from Lutetia.

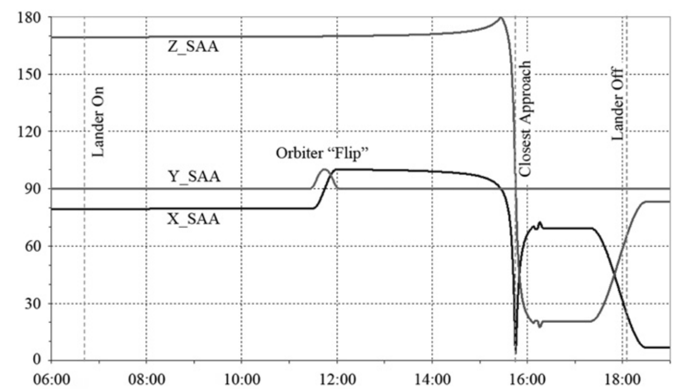

Fig. 3. Rosetta spacecraft orientation during the flyby. Y-axis was constant through-out the flyby and parallel to solar illumination. Before the sub-solar point the $-Z$-panel received the greatest amount of illumination whilst the $-X$-panel received a small and decreasing illumination and the $+X$-panel was in shadow. After the sub-solar point the $+X$-panel is illuminated and the $+Z$-panel becomes illuminated shortly after close approach, this rapidly changing orientation occurring in a time of about 30 min.

the sub-solar point the $-Z$-panel receives almost constant illumination with the $+X$-panel receiving a small and gradually decreasing insolation. After the sub-solar point the $-X$-panel (on which the Lander is attached) began to become illuminated, reaching a maximum at CA, whereupon the $+Z$-panel started to become illuminated. Thus out-gassing was expected to increase and reach a maximum around CA.

The spacecraft orientation resulted in the Lander being exposed to direct solar illumination for an extended period of time before CA. Since the Lander was designed to operate at 3.0 AU within the dusty environment of a comet it is insulated to such an extent that modelling showed that even at the distance of 2.7 AU it could exceed its maximum operating temperature. During the long-distance observations of Lutetia, prior to CA − 4 h, the spacecraft was periodically pointed away from Lutetia such that the Lander was in shadow (as in normal flight operations), to prevent overheating. The periods when the Lander was illuminated also helped to remove condensed surface volatiles accumulated during the Cruise Phase when the Lander was permanently in shadow. During the encounter the Lander power was kept to a minimum and the Lander was switched off at CA + 1 h.

The instruments on Rosetta are broadly split into two classes: the remote sensing instruments (Alice and MIRO) and the in-situ instruments (RPC, ROSINA, Ptolemy and COSAC). In general the remote sensing instruments are tuned to detect specific molecules and measure the column density of the target molecules to derive a global out-gassing rate for the asteroid, whereas the in-situ instruments measure the density (often converted to pressure) of the exosphere at the spacecraft location and are more sensitive to local variations in the exosphere structure. The mass spectrometers can also measure the composition giving the possibility of distinguishing between different sources such as sublimation, micrometeorite sputtering and spacecraft effects.

The high flyby speed of 15 km s^{-1} of Rosetta during the Lutetia flyby has a major advantage in that any detection would be for a very short time near CA with the high speed creating a pressure ram effect on the forward face of the spacecraft and enhancing the sensitivity for the mass spectrometer and pressure sensing instruments ROSINA, Ptolemy and COSAC (Wurz et al., 2007). The average molecular speed is given as $v = (8\,k_B\,T/\pi\,m)^{0.5}$ (Delchar, 1993), where T is the temperature, m is the mass of the molecule and k_B is the Boltzmann constant (1.38×10^{-23} J K^{-1}). At a temperature of 240 K water has an average speed of approximately 530 m s^{-1}, so giving an effective pressure increase during the asteroid approach of $(v_s \cos\alpha + 0.53)/0.53$, where v_s is the spacecraft velocity and α is the spacecraft Z-axis phase angle. The effective pressure increase for small values of α would be about

30; this is even further enhanced for heavier, although probably less abundant, molecules.

Details of the types of instrument and their capabilities for detecting and analysing the exosphere are briefly described in the sub-sections below. A summary of each instrument's capabilities of detection limit is shown in Table 1.

2.1. Mass spectrometers and pressure sensor

There are a total of four mass spectrometers: two on the orbiter as part of the ROSINA instrument (a Double-Focussing Mass Spectrometer (DFMS), and the Rosetta Time-Of-Flight mass spectrometer (RTOF;) Balsiger et al., 2009) and two on the Philae lander; COSAC (Goesmann et al., 2009) and Ptolemy (Morse et al., 2009). The ROSINA instrument includes a pressure sensor (the Comet Pressure Sensor (COPS)). All these instruments measure the gas pressure in-situ with the mass spectrometers measuring gas composition. Both of the orbiter mass spectrometers point along the $+Z$ axis and gain from the ram effect. The two Lander instruments are designed to measure comet solid samples by GC–MS; however in the absence of helium carrier gas they operate in "sniff mode", monitoring the external environment via helium vent pipes. An overview of the mass spectrometer capabilities is shown in Table 1.

ROSINA operations during Lutetia flyby consisted in operating all three instruments but with some modification (described in full in Altwegg et al., 2012). The high speed encounter with Lutetia did not allow adequate time for the DFMS to scan a full mass spectrum, so it was operated at a single peak, mass 18, with a collection time of 10 s. Meanwhile RTOF was reserved for operation closer to the asteroid since high voltage flash-over problems earlier in the mission were resolved only just prior to the flyby. Unfortunately due to the changes in operational procedures and software use, DFMS and COPS were unintentionally switched off during the CA. However DFMS measurements made before and after the spacecraft flip indicate that the water pressure from the spacecraft was gradually increasing throughout the close encounter; this was used to calibrate RTOF. Just before CA, RTOF detected an increase in water signal equivalent to $1.8(\pm 0.5)\times 10^5\ \mathrm{cm}^{-3}$ exactly as expected for an exosphere, which was not observed during the Lutetia rehearsal. However out-gassing from the spacecraft could not be ruled out and so this does not constitute a positive detection (Altwegg et al., 2012).

The Lander mass spectrometers operations during the Lutetia encounter (Andrews et al., 2012; Goesmann et al., 2012) consisted of 5 discrete blocks of measurements each lasting a couple of minutes at approximately hourly intervals. The measurements before and after CA were used to monitor the background contamination, whilst the third measurement at CA$-$17 min measured background plus any exosphere above the sub-solar point. The location of the COSAC vent pipe precluded direct measurement of any exosphere from Lutetia: during the approach it was facing away from the asteroid and after the flyby the spacecraft speed was much faster than that of the gas flow from Lutetia. However the opportunity of the flyby was used to operate at CA$-$3 h and CA$+$1 h with the aim of monitoring the internal Lander environment and simultaneous measurements provided a cross calibration between the other mass spectrometers. Both mass spectrometers measured increasing pressure with increasing instrument temperature during the encounter, but Ptolemy indicated an additional 10% increase at the third measurement, equivalent to the pressure increasing by 1.7×10^{-10} mbar. However the spectra at CA$-$17 min showed no significant difference between the background measurements, so Ptolemy was unable distinguish whether the increase was caused by an increase in spacecraft out-gassing or an exosphere consisting of mainly water.

2.2. RPC and ROMAP magnetometers

The Rosetta Plasma Consortium (RPC) consists of a suite of 5 instruments designed to measure the local plasma environment (Carr et al., 2009). An exosphere could be detected by an increase in ion concentration with a detection limit of $\sim$1 ion cm^{-3} as it is ionised by the solar wind and also by its effect on the magnetic field of Lutetia, similar to the effects that led to the detection of an atmosphere from Enceladus (Dougherty et al., 2006). The Lander has a separate magnetometer instrument, ROMAP (Auster et al., 2009) for measurements close to and on the surface of the comet. During the Cruise Phase, measurements in parallel with RPC compensate for spacecraft disturbances, especially from the Lander during active phases.

The main objective of RPC was to measure the magnetic field of Lutetia and determine whether it contained a magnetic core. To this end the main instrument deployed during flyby was RPC-MAG (Glassmeier et al., 2009b) with ROMAP, operational for ± 3 days (equivalent to $\pm$40,00,000 km) on either side of CA

Table 1
Summary of instrument capabilities.

Instrument	Type	Measurement		Detection limit
		Type	Details	
ROSINA COPS	In-situ	Pressure	Sampling period 10 s	10^5 cm^{-3} ($\sim 4\times 10^{-11}$ mbar)
ROSINA DFMS	In-situ	Pressure and composition m/z 12–150 Da[a]	Sampling period 30 min Orbiter $+Z$ pointing ram enhancement	1 cm^{-3} ($\sim 4\times 10^{-16}$ mbar)
ROSINA RTOF	In-situ	Pressure and composition m/z 1–300 Da	Sampling period 200 s Orbiter $+Z$ pointing ram enhancement	10^2 cm^{-3} ($\sim 4\times 10^{-14}$ mbar)
Ptolemy	In-situ	Pressure and composition m/z 11–142 Da	Sampling period 135 s Lander, vent pipe $+Z$ pointing, ram enhancement	1×10^{-10} mbar
COSAC	In-situ	Pressure and composition	Sampling period 126 s Lander, vent pipe $-Z$ pointing	1×10^{-10} mbar
RPC-MAG ROMAP	In-situ	Plasma environment	Magnetic field	0.04 nT
Alice	Remote	Hα	Global density	1×10^{26} molecules s^{-1}
MIRO	Remote	Water	Column density	8.1×10^{12} molecules cm^{-2}
		Ammonia		4.0×10^{13} molecules cm^{-2}
		Carbon monoxide and		1.3×10^{15} molecules cm^{-2}
		Methanol		1.2×10^{15} molecules cm^{-2}

[a] 1 Da is equivalent to 1 amu.

(Richter et al., 2012). RPC-IES did not operate due to unfavourable pointing conditions. The measured magnetic influence of Lutetia at 3160 km was well below 1 nT, if any. Modelling of the effect of an exosphere indicated that even an exosphere of 3.2×10^{25} molecules s^{-1} would have an undetectable effect on the magnetic field at the flyby distance of 3160 km.

2.3. Alice

The Alice instrument (Parker et al., 2009) is an ultraviolet (UV) imaging spectrograph with a spectral range of 700–2050 Å. The detector has a 5.5° span, split into 20 channels. The central portion of the slit (2° span) has a 0.05° width with the remaining slit having a 0.1° width. An exosphere can be detected by the resonant scattering of sunlight by H (with the H_I Lyα at 1216 Å) and O (with the O_I multiplet at 1304 Å), these being produced by the dissociation of water.

During the approach to Lutetia, Alice collected data over a period of 20.2 h at a spacecraft distance of 2.7×10^6 km–1.2×10^6 km (Stern et al., 2011). The only features detected were H Lyα and Lyβ lines. Comparison with spectra obtained after CA viewing the same area of sky without Lutetia in the field of view showed no difference, indicating that these features were solely due to H in the interplanetary medium. The detection limit of H from Lutetia was $<7\times10^9$ cm^{-2}, which corresponds to a production rate of water $<1.0\times10^{26}$ molecules s^{-1}.

2.4. MIRO

The MIRO instrument (Gulkis et al., 2007) consists of two heterodyne radiometers with centre-band operating frequencies near 190 GHz (1.6 mm) and 562 GHz (0.5 mm). Broadband continuum channels are implemented in both frequency bands for the measurement of near surface temperatures. A very high spectral resolution spectrometer (44 kHz) is interfaced with the 562 GHz, submillimeter radiometer. The submillimeter radiometer/spectrometer is fixed-tuned to measure simultaneously four volatile species—CO, CH_3OH, NH_3 and three isotopes of water, $H_2^{16}O$, $H_2^{17}O$ and $H_2^{18}O$. The half-power beam width of the instrument is 7.5' at 562 GHz. Minimum detectable column densities to produce a 2 K signal in the spectrometer, a signal strength obtainable in about 20 min of integration time, are 8×10^{12} molecules cm^{-2} for water and 1.3×10^{15} molecules cm^{-2} for carbon monoxide. The estimates assume a rotational temperature of 300 K.

MIRO made continuum measurements of the near surface temperature of Lutetia during the flyby providing information concerning the properties of Lutetia that affect out-gassing (Gulkis et al., 2012). Owing to the high relative velocity of the spacecraft and Lutetia, the Doppler shifted spectral lines of water were only within the passband of the receiver for ~5 min either side of CA. The search for water consisted of combining 7 spectra each of 30 s duration around CA. No signals were detected above a 3 sigma noise level, giving an upper limit for the column density of water of 5×10^{11} molecules cm^{-2}.

3. Discussion

3.1. Comparison of instrument sensitivity

The results from the various instruments (as given in the special issue) are expressed in units specific to each type of measurement/instrument. As such a direct comparison between the data is not straightforward. In this section a simple model of an asteroid exosphere is used in order to allow comparisons between the instruments and calculate their detection limit. The main component is assumed to be water released by sublimation at a temperature of 240 K and expanding outwards homogenously (i.e. pressure decreasing outwards according to a $1/r^2$ relationship). Other production mechanisms, such as ion sputtering by the solar wind and micrometeorite vaporization, were investigated by Schläppi et al. (2008), but the maximum density of 10^3 particles m^{-3} at the flyby distance would be below detection limits.

For a production rate Q in molecule s^{-1}, the number density N at a distance r from the asteroid centre is given by

$$N = Q/(4\pi r^2 v)\ [\text{molecules}\,\text{m}^{-3}] \tag{1}$$

The pressure P is given from the ideal gas law, where $P=Nk_BT$; hence

$$P = Qk_BT/(4\pi r^2 v)\ [\text{Pa}] \tag{2}$$

In the case of the ROSINA instruments and Ptolemy the pressure measured by the instrument, P_{inst}, is enhanced by the ram effect, as discussed in Section 2:

$$P_{inst} = P(v_s \cos\alpha + v)/v\ [\text{Pa}] \tag{3}$$

Molecules from Lutetia are ionised by photo-ionisation and interaction with the solar wind with an ionisation scale length at 2.7 AU of 7.3×10^6 km (Hansen et al., 2009). The fraction of molecules ionised is $1-\exp(-r/\lambda)$. Hence, the number of ions at distance r is given by

$$N_{ion}(r) = (1-\exp(-r/\lambda))Q/(4\pi r^2 v)\ [\text{ions}\,\text{m}^{-3}] \tag{4}$$

MIRO measures the column density, N_{col}, at a distance r, as given by

$$N_{col} = Q/(4\pi v)\int_{r_a}^{r}\frac{1}{r^2}\,dr\ \left[\text{molecules}\,\text{m}^{-2}\right] \tag{5}$$

where r_a is the radius of the asteroid. Since the spacecraft flyby distance $r \gg$ the exosphere scale height, the detection limit is close to

$$N_{col} = Q/(4\pi r_a v)\ [\text{molecules}\,\text{m}^{-2}] \tag{6}$$

A comparison of the exosphere production rate required for detection by each instrument against distance from the asteroid is shown in Fig. 4. Values were calculated using the simple model described above and using the instrument detection limits in Table 1. An effective detection limit of 10^{-12} mbar was used for the ROSINA RTOF and DFMS mass spectrometers because their sensitivity was reduced by spacecraft out-gassing.

Of interest for the comet encounter is the detection limit of carbon monoxide. In general, the sensitivity of the mass spectrometers (RTOF, DFMS, COSAC and Ptolemy) is increased by a factor of 12 since they are (a) more sensitive to CO, because it is a smaller component of the spacecraft background and (b) have an enhanced signal from the ram effect, which is increased by ~25% with respect to water because of the higher molecular mass of CO compared to H_2O. In contrast, the sensitivity of MIRO for CO is lower by factor 150. These results are summarised in Table 2. None of the instruments detected any indication of CO, giving a global production rate of $<1.7\times10^{25}$ molecules s^{-1}.

3.2. Combining instrument results

For most cases the presence of any exosphere was below detection limits, taking the results from MIRO, the most sensitive instrument, and assuming the simple out-gassing model described above, then the water production rate is $<4.3\times10^{23}$ molecules s^{-1}. However for the two mass spectrometers that were in operation near CA (RTOF and Ptolemy) there was an apparent increase in water pressure. Whilst recognising that this is probably due to spacecraft out-gassing, it is instructive for future comet operations to look at combining the individual results and investigating what constraints this implies for an exosphere.

A direct comparison of the mass spectrometer results is shown in Fig. 5. Ptolemy only made a single measurement near CA at the sub-solar point; however, the more sensitive ROSINA instrument did not detect a simultaneous pressure increase, thus suggesting that the Ptolemy measurement was more likely to be due to pressure changes within the Lander environment. The pressure rise measured by ROSINA (inset Fig. 5) shortly before Close Approach was consistent with an exosphere and the measurement was made when it had a sensitivity similar to those of Alice and RPC-MAG (Fig. 4), with a detection limit of 1×10^{26} molecules s^{-1} (~ 3 kg s^{-1}) equivalent to those of low activity comets. One possibility is that the out-gassing is not homogenous but concentrated in jets similar to comets, e.g. EPOXI observed jets of water not associated with dust jets (A'Hearn, 2010). A similar effect could be occurring on asteroids, albeit at a lower intensity. The orientation of Lutetia results in the sunlit pole being strongly heated compared to the unlit side, so some directional plume would be expected. Alternatively recent cratering may have exposed buried ice, which could result in a localised water emission.

A more rigorous model for directional out-gassing by sublimation (Altwegg et al., 2012) estimated a production rate of $(3.2 \pm 1.6) \times 10^{25}$ molecules s^{-1} ($\sim 1 \pm 0.5$ kg s^{-1}). Still above the detection limit of MIRO, but as indicated in Fig. 6, localised active regions could have been missed by MIRO, which has a narrow footprint of about 7 km diameter and was able to detect water only when Rosetta was ~ 1600 km from CA. Any increase in sensitivity from directional out-gassing would also increase sensitivity for RPC-MAG and Alice. The detection limit of RPC-MAG assumed that the magnetic field strength of Lutetia was 1 nT at 3160 km; a lower magnetic field would reduce the sensitivity. Furthermore, observations of both RPC-MAG and Alice depend on the extent of dissociation of water into H and O ions by the solar wind, which is variable, so the possibility remains that

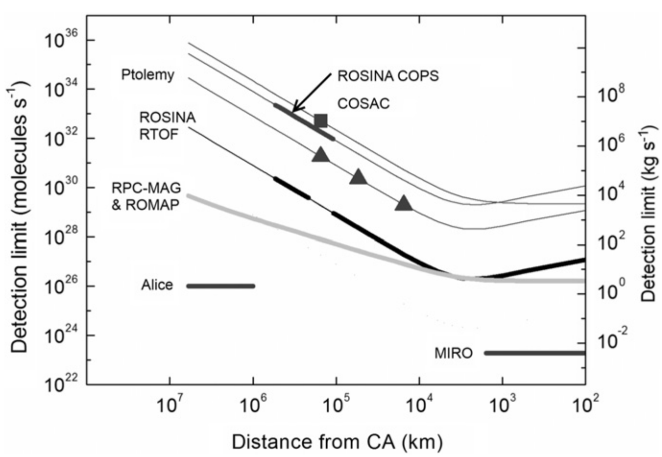

Fig. 4. Comparison of the instrument sensitivity against distance from the asteroid. The in-situ instruments had the greatest sensitivity at ~ 3000 km before CA because of the ram effect. Solid lines and points indicate when instruments were making measurements. Values are calculated from the instrument sensitivity in Table 1, using equations in Section 3.1 as follows: COSAC—Eq. (2), RTOF and Ptolemy—Eqs. (2) and (3), RPC-MAG—Eq. (4) and MIRO—Eq. (5). A detection value 1×10^{12} mbar is used for RTOF because the sensitivity was limited by spacecraft background.

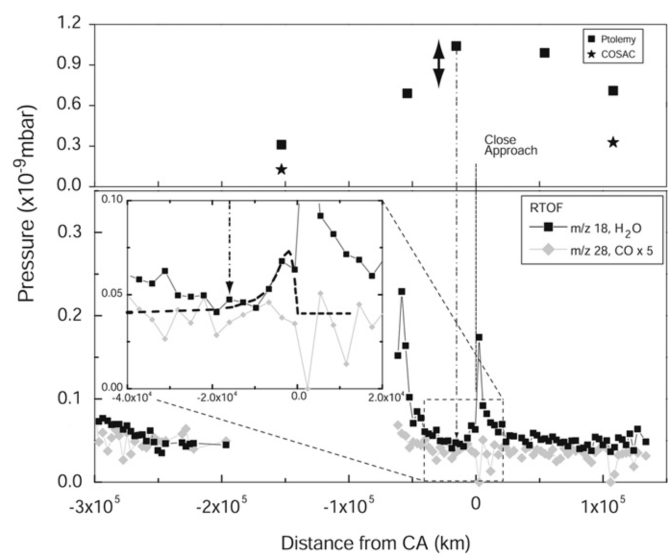

Fig. 5. Comparison of the mass spectrometer data for ROSINA RTOF, COSAC and Ptolemy (RTOF CO data from K. Altwegg, pers. comm.). Both Ptolemy and COSAC show an increase in their first and last measurements by a factor of 2, consistent with an increased pressure as the Lander became warmer. The pressure enhancement of 0.2×10^{-9} mbar measured by Ptolemy at 15,500 km before CA (indicated by the arrowed line) was not observed by ROSINA RTOF, suggesting that this was caused by local spacecraft effects. The inset shows an expanded view of the Rosina RTOF data just before CA. The dashed line is the predicted RTOF water signal for a Lutetia production rate of 2×10^{26} molecules s^{-1} in addition to a spacecraft background of 4×10^{-11} mbar.

Table 2
Lutetia exosphere measurements. MIRO is the most sensitive instrument in detecting water. For CO the mass spectrometer sensitivity is increased by 12 because of lower background and increased ram effect. The most sensitive instrument RTOF did not detect any CO (Fig. 5).

Instrument	Measurement details			Global production rate (molecules s^{-1})
	Component	Measurement	Distance to asteroid centre (km)	
ROSINA-COPS	Total	$< 4 \times 10^{-14}$ mbar	54,000	$< 2.0 \times 10^{27}$
ROSINA-DFMS	H_2O	$< 4 \times 10^{-14}$ mbar	54,000	$< 1.7 \times 10^{27}$
ROSINA-RTOF	H_2O	$< 4 \times 10^{-14}$ mbar	3800	$< 2.0 \times 10^{26}$
	CO	$< 3 \times 10^{-15}$ mbar	3800	$< 1.7 \times 10^{25}$
Ptolemy	H_2O	$< 4 \times 10^{-12}$ mbar	15,500	$< 2.0 \times 10^{29}$
	CO	$< 3 \times 10^{-13}$ mbar	15,500	$< 1.7 \times 10^{28}$
RPC-MAG/ROMAP	Total	< 1 nT	3162	$< 3.2 \times 10^{25}$ (from hybrid simulations)
Alice	H_2O	$< 1 \times 10^{26}$ mol s^{-1}	$> 10,00,000$	$< 1.0 \times 10^{26}$
MIRO	H_2O	8.1×10^{12} mol m^{-2}	< 5000	$< 4.3 \times 10^{23}$
	CO	1.3×10^{15} mol m^{-2}	< 5000	$< 6.9 \times 10^{25}$

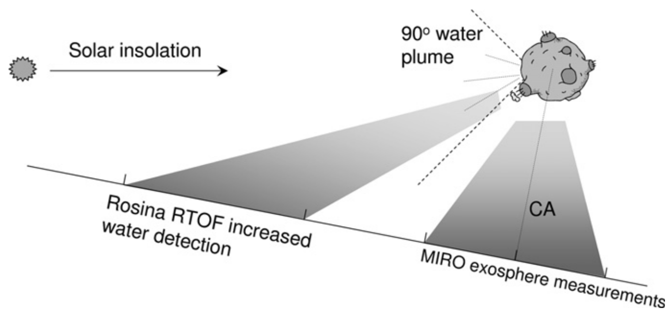

Fig. 6. A schematic diagram showing the Luetia flyby geometry and instrument operations. MIRO, the instrument most sensitive to water, did not detect any water; however it has a small beam diameter of about 7 km and only measured 1575 km on either side of CA. ROSINA RTOF detected an increase in water before CA when it was most sensitive to the exosphere because of a combination of distance to the asteroid and the ram effect. A directional plume of water with an angular width of 90° and production rate of 1.5×10^{25} molecules s^{-1} ($\sim$0.5 kg s^{-1}) could have been detectable by ROSINA RTOF but not by MIRO.

the amount observed by ROSINA may have been below their detection limit.

3.3. Future activities

One of the goals of the Rosetta mission is to study the structure and chemical composition of the comet coma and its evolution as the comet approaches perihelion. At an initial comet encounter distance of 3.5 AU from the Sun, the gas production rate is estimated to be of the order of 6×10^{26} molecules s^{-1} (De Sanctis et al., 2010). During the mapping phase of the mission Rosetta will orbit the comet at a distance of 100 km, decreasing to 20 km, so all instruments will have sufficient sensitivity to measure the coma. However, the main lesson learnt from the asteroid encounters is that sensitivity is limited by spacecraft out-gassing rather than instrument sensitivity (Schläppi et al., 2010). Rosetta will be immersed within the coma with no possibility to make background measurements, so it will be important to have a better understanding of spacecraft out-gassing and limiting its effects. An opportunity to make background measurements at various spacecraft orientations arises shortly after hibernation whilst Rosetta is more than 10^6 km from the comet. These measurements would also help remove volatiles that have condensed during hibernation from all of the spacecraft panels. Once at the comet, measurements of the coma structure will benefit by having dedicated sessions for the in-situ instruments with the spacecraft maintaining a constant solar angle for a period of at least 4 h as it passes through active regions. Combined operations will enable cross calibration between the instruments to enable direct comparison of results between the Orbiter instruments and the Lander instruments on the comet surface.

4. Conclusions

The Rosetta flyby of Lutetia provided an opportunity for seven instruments to make a co-ordinated campaign to determine the existence, composition and structure of an exosphere. The final asteroid flyby sequence involved incorporation of experience gained during the Steins encounter, tests during rehearsal to ascertain instrument interferences and detailed planning similar to that expected at comet encounter. Overall the operation of all the instruments performed as expected; the anomalies that did occur can be corrected for future operations.

None of the instruments detected an unambiguous signal of an exosphere. Assuming a spherical source, the production rate of water $<4.3\times10^{23}$ molecules s^{-1} and carbon monoxide $<1.7\times10^{25}$ molecules s^{-1}. The cause of the tantalising increase in water detected by ROSINA RTOF remains ambiguous, and could be either from an exosphere or simply due to spacecraft out-gassing. However the lack of a water signal detection by the more sensitive MIRO indicates that if this was due to an exosphere then the water out-gassing is directional with a half-width angle $<90^\circ$ and a production rate of water of 1.5×10^{25} molecules s^{-1} or less. RPC-MAG measurement revealed an asteroid influence on the magnetic field of less than 1 nT at 3160 km.

During the initial comet encounter at 3.5 AU, the expected production rate is of the order 6×10^{26} molecules s^{-1} (De Sanctis et al., 2010). All the instruments will have sufficient sensitivity to analyse the coma, since Rosetta will initially be orbiting much closer at a distance of 100 km, reducing over a period of a few months to 20 km. However experience gained from the Lutetia encounter shows that distinguishing spacecraft effects will be more difficult at the comet as Rosetta will be immersed within the coma, so there will be no way to measure background levels and no sensitivity increase due to the ram effect. Measurements made shortly after hibernation will help characterisation of the spacecraft out-gassing and dedicated coma analysis sequences will help reduce the background. Complementary measurements between instruments during the initial orbits will enhance measurements made once the Philae Lander is on the comet surface, where joint measurements will provide data on two locations simultaneously.

The Rosetta spacecraft has now entered its hibernation phase until comet approach in January 2014. During this time more information concerning small Solar System bodies will continue to be gathered with the imminent arrival of the Dawn spacecraft at Vesta followed by its arrival at Ceres a year later.

Acknowledgements

We gratefully acknowledge the help of many individuals who have made this work possible, the co-ordination and operation of seven instruments onboard the Rosetta mission: Alice, COSAC, MIRO, RPC, ROMAP ROSINA and Ptolemy. Instrument team members included H. Balsiger, S.J. Barber, J-L. Bertax, J.J. Berthelier, E. Birath, J.H. Bredehöft, U. Calmonte, N. Cunningham, J.De Keyser, L. Feaga, B. Fiethe, S. Fuselier, K.-H. Glassmeier, A. Graps, M. Hässig, L. Hofer, A. Jäckel, C. Koenders, M.R. Leese, U. Mall, S. McKenna-Lawlor, U. Meierhenrich, G.H. Morgan, U. Motschmann, J. Müller, G.M. Muñoz-Caro, C.T. Pillinger, F. Raulin, H. Rème, R. Roll, M. Rubin, J.R. Scherrer, B. Schläppi, D.C. Slater, A. Steffl, C. Szopa, W. Thiemann, M. Versteeg, P. Wurz and J.C. Zarnecki. Thanks must go to the teams at the Rosetta Mission Operations Centre, the Centre National d'Études Spatiales and the Deutschen Zentrums für Luft- und Raumfahrt for their operational support.

References

Accomazzo, A., Ferri, P., Lodiot, S., Hubault, A., Porta, R., Pellon-Bailon, J.-L., 2010. The first Rosetta asteroid flyby. Acta Astronomica 66, 382–390.
A'Hearn, M.F., 2010. EPOXI: Two intriguing investigations—one flight-proven spacecraft. ⟨http://epoxi.umd.edu/⟩ (accessed May, 2011).
Altwegg, K., Balsiger, H., Calmonte, U., Hässig, M., Hofer, L., Jäckel, A., Schläppi, B., Wurz, P., Berthelier, J.J., De Keyser, J., Fiethe, B., Fuselier, S., Mall, U., Rème, H., Rubin, M., 2012. In situ mass spectrometery during the Lutetia flyby. Planetary and Space Science 66, 173–178.
Andrews, D.J., Morse, A.D., Barber, S.J., Leese, M.R., Morgan, G.H., Sheridan, S., Zarnecki, J.C., Pillinger, C.T., Wright, I.P., 2012. Ptolemy operations and results from the Lutetia flyby. Planetary and Space Science 66, 179–186.

Auster, H.U., Apathy, I., Berghofer, G., Remizov, A., Roll, R., Fornacon, K.H., Glassmeier, K.H., Haerendel, G., Hejja, I., Kührt, E., Magnes, W., Moehlmann, D., Motschmann, U., Richter, I., Rosenbauer, H., Russell, C.T., Rustenbach, J., Sauer, K., Schwingenschuh, K., Szemerey, I., Waesch, R., 2009. Rosetta Magnetometer and plasma monitor onboard the Rosetta Lander. In: Schulz, R., Alexander, C., Boehnhardt, H., Glassmeier, K.-H. (Eds.), Rosetta, ESA's Mission to the Origin of the Solar System. Springer, pp. 701–718.

Barucci, M.A., Fulchignoni, M., 2009. Pre-fly-by properties of the Rosetta asteroids targets 2867 Steins and 21 Lutetia. In: Schulz, R., Alexander, C., Boehnhardt, H., Glassmeier, K.-H. (Eds.), Rosetta, ESA's Mission to the Origin of the Solar System. Springer, pp. 55–68.

Balsiger, H., Altwegg, K., Bochsler, P., Eberhardt, P., Fischer, J., Graf, S., Jäckel, A., Kopp, E., Langer, U., Mildner, M., Müller, J., Riesen, T., Rubin, M., Scherer, S., Wurz, P., Wüthrich, S., Arijs, E., Delanoye, S., De Keyser, J., Neefs, E., Nevejans, D., Rème, H., Aoustin, C., Mazelle, C., Médale, J.-L., Sauvaud, J.A., Berthelier, J.-J., Bertaux, J.-L., Duvet, L., Illiano, J.-M., Fuselier, S.A., Ghielmetti, A.G., Magoncelli, T., Shelley, E.G., Korth, A., Heerlein, K., Lauche, H., Livi, S., Loose, A., Mall, U., Wilken, B., Gliem, F., Fiethe, B., Gombosi, T.I., Block, B., Carignan, G.R., Fisk, L.A., Waite, J.H., Young, D.T., Wollnik, H., 2009. Rosetta orbiter spectrometer for ion and neutral analysis ROSINA. In: Schulz, R., Alexander, C., Boehnhardt, H., Glassmeier, K.-H. (Eds.), Rosetta, ESA's Mission to the Origin of the Solar System. Springer, pp. 485–536.

Campins, H., Hargrove, K., Pinilla-Alonso, N., Howell., E.S., Kelley, M.S., Licandro, J., Mothé-Diniz, T., Fernández, Y., Ziffer, J., 2010. Water ice and organics on the surface of the asteroid 24 Themis. Nature 464, 1320–1321.

Carr, C., Cupido, E., Lee, C.G.Y., Balogh, A., Beek, T., Burch, J.L., Dunford, C.N., Eriksson, A.I., Gill, R., Glassmeier, K.H., Goldstein, R., Lagoutte, D., Lundin, R., Lundin, K., Lybekk, B., Michau, J.L., Musmann, G., Nilsson, H., Pollock, C., Richter, I., Trotignon, J.G., 2009. RPC: The Rosetta Plasma Consortium. In: Schulz, R., Alexander, C., Boehnhardt, H., Glassmeier, K.-H. (Eds.), Rosetta, ESA's Mission to the Origin of the Solar System. Springer, pp. 383–398.

Carry, B., Kaasalainen, M., Leyrat, C., Merline, W.J., Drummond, J.D., Conrad, A., Weaver, H.A., Tamblyn, P.M., Chapman, C.R., Dumas, Colas, C.F., Christou, J.C., Dotto, E., Perna, D., Fornasier, S., Bernasconi, L., Behrend, R., Vachier, F., Kryszczynska, A., Polinska, M., Fulchignoni, M., Roy, R., Naves, R., Poncy, R., Wiggins, P., 2010. Physical properties of the ESA Rosetta target asteroid (21) Lutetia. Astronomy and Astrophysics 523, A94.

Delchar, T.A., 1993. Vacuum Physics and Techniques. Chapman and Hall.

De Sanctis, M.C., Lasue, J., Capria, M.T., Magni, G., Turrini, D., Coradini, A., 2010. Shape and obliquity effects on the thermal evolution of the Rosetta target 67P/Churyumov–Gerasimenko cometary nucleus. Icarus 207, 341–358.

Dougherty, M.K., Khurana, K.K., Neubauer, F.M., Russell, C.T., Saur, J., Leisner, J.S., Burtom, M.E., 2006. Identification of a dynamic atmosphere at Enceladus with the Cassini magnetometer. Science 311, 1406–1409.

Graf, S., Altwegg, K., Balsiger, H., Bochsler, P., Fiethe, B., Montagnon, E., 2008. Thruster plumes: sources for high pressure and contamination at the payload location. Journal of Spacecraft and Rockets 45 (1), 57–64.

Glassmeier, K.-H., Boehnhardt, H., Koschny, D., Kührt, E., Richter, I., 2007. The ROSETTA mission: flying towards the origin of the solar system. Space Science Reviews 128, 1–21.

Glassmeier, K.-H., Boehnhardt, H., Koschny, D., Kührt, E., Richter, I., 2009a. The Rosetta mission: flying towards the origin of the solar system. In: Schulz, R., Alexander, C., Boehnhardt, H., Glassmeier, K.-H. (Eds.), Rosetta, ESA's Mission to the Origin of the Solar System. Springer, pp. 1–20.

Glassmeier, K.-H., Richter, I., Musmann, G., Auster, H.-U., Motschmann, U., Balogh, A., Carr, C., Cupido, E., Coates, A., Rother, M., Schwingenschuh, K., Stoll, B., Szegö, K., Tsurutani, B., 2009b. The Rosetta Orbiter Fluxgate Magnetometer. In: Schulz, R., Alexander, C., Boehnhardt, H., Glassmeier, K.-H. (Eds.), Rosetta, ESA's Mission to the Origin of the Solar System. Springer, pp. 449–471.

Goesmann, F., Rosenbauer, H., Roll, R., Szopa, C., Raulin, F., Sternberg, R., Israel, G., Meierhenrich, U., Thiemann, W., Munoz-Caro, G., 2009. COSAC, The Cometary Sampling and Composition Experiment on Philae. In: Schulz, R., Alexander, C., Boehnhardt, H., Glassmeier, K.-H. (Eds.), Rosetta, ESA's Mission to the Origin of the Solar System. Springer, pp. 633–650.

Goesmann, F., McKenna-Lawlor, S., Reinhard, R., Bredehöft, J.H., Meierhenrich, U., Raulin, F., Thiemann, W., Munoz-Caro, G.M., Szopa, C., 2012. Interpretation of COSAC mass spectrometer data acquired during Rosetta's Lutetia fly-by 10th of July 2010. Planetary and Space Science 66, 187–191.

Gulkis, S., Frerking, M., Crovisier, J., Beaudin, G., Hartogh, P., Encrenaz, P., Koch, T., Kahn, C., Salinas, Y., Nowicki, R., Irigoyen, R., Janssen, M., Stek, P., Hofstadter, M., Allen, M., Backus, C., Kamp, L., Jarchow, C., Steinmetz, E., Deschamps, A., Krieg, J., Gheudin, M., Bockelée-Morvan, D., Biver, N., Encrenaz, T., Despois, D., Ip, W., Lellouch, E., Mann, I., Muhleman, D., Rauer, H., Schloerb, P., Spilker, T., 2007. MIRO: microwave instrument for Rosetta Orbiter. Space Science Review 128, 561–597.

Gulkis, S., Keihm, S., Kamp, L., Lee, S., Hartogh, P., Crovisier, J., Lellouch, E., Encrenaz, P., Bockelée-Morvan, D., Hofstadter, M., Beaudin, G., Janssen, M., Weissman, N., von Allmen, P., Encrenaz, T., Backus, C., Ip, W.-H., Schloerb, P., Biver, N., Spilker, T., 2012. Continuum and spectroscopic observations of asteroid (21) Lutetia at millimeter and submillimeter wavelengths with the MIRO instrument on the Rosetta Spacecraft. Planetary and Space Science 66, 31–42.

Hansen, K.C., Bagdonat, T., Motschmann, U., Alexander, C., Combi, M.R., Cravens, T.E., Gombosi, T.I., Jia, Y.-D., Robertson, I.P., 2009. The plasma environment of copet 67P/Churyumov–Gerasimenko throughout the Rosetta mission. In: Schulz, R., Alexander, C., Boehnhardt, H., Glassmeier, K.-H. (Eds.), Rosetta, ESA's Mission to the Origin of the Solar System. Springer, pp. 69–98.

Hsieh, H.H., Jewitt, D.C., Fernández, Y.R., Yanga R., 2004. The strange case of 133P/Elst-Pizarro: a comet among the asteroids. Astronomical Journal 127, 2997–3017.

Hsieh, H.H., Jewitt, D., 2006. A population of comets in the main asteroid belt. Science 312, 516–563.

Hsieh, H.H., Jewitt, D., Lacerda, P., Lowry, S.C., Snodgrass, C., 2010. The return of activity in main-belt comet 133P/Elst–Pizarro. Monthly Notices of the Royal Astronomical Society 403, 363–377.

Jäckel, A., Schläppi, B., Altwegg, K., Balsiger, H., 2009. Discussion of ROSINA-COPS measurements during the (2867) Steins flyby. EPSC Abstracts 4, EPSC 2009-505.

Jewitt, D., Weaver, H., Agarwal, J., Mutchler, M., Drahus, M., 2010. A recent disruption on the main-belt asteroid P/2010 A2. Nature 467, 817–819.

Landsman, Z., Licandro, J., Campins, H., Kelley, M., Hargrove, K., Pinilla-Alonso, N., Cruikshank, D., Rivkin, A.S., Emery, J., 2010. Asteroid 65 Cybele: detection of small silicate grains, water-ice and organics. Bulletin of the American Astronomical Society 42, 1035.

Morse, A.D., Morgan, G.H., Andrews, D.J., Barber, S.J., Leese, M.R., Sheridan, S., Wright, I.P., Pillinger, C.T. 2009. Ptolemy — a GCMS to measure the chemical and stable isotopic composition of a comet. In: Schulz, R., Alexander, C., Boehnhardt, H., Glassmeier, K.-H. (Eds.), Rosetta, ESA's Mission to the Origin of the Solar System. Springer, pp. 669–686.

Parker, J.Wm, Stern, S.A., Slater, D.C., Scherrer, J., Stone, J., Versteeg, M., Steffl., A.J., A'Hearn, M.F., Bertaux, J.L., Feldman, P.D., Festou, M.C., Weaver, H.A., Siegmund, O.H.W., 2009. Alice: The Rosetta ultraviolet imaging spectrograph. In: Schulz, R., Alexander, C., Boehnhardt, H., Glassmeier, K.-H. (Eds.), Rosetta, ESA's Mission to the Origin of the Solar System. Springer, pp. 167–182.

Richter, I., Auster, H.U., Glassmeier, K.-H., Koenders, C., Carr, C.M., Motschmann, U., Müller, J., McKenna-Lawlor, S., 2012. Magnetic field measurements during the ROSETTA flyby at asteroid (21) Lutetia. Planetary and Space Science 66, 155–164.

Rivkin, A.S., Emery, J.P., 2010. Detection of ice and organics on an asteroidal surface. Nature 464, 1322–1323.

Rivkin, A.S., Howell, E.S., Britt, D.T., Lebofsky, L.A., Nolan, M.C., Branston, D.D., 1995. 3 μm spectrophotometric survey of M- and E-class asteroids. Icarus 117, 90–100.

Rivkin, A.S., Howell, E.S., Lebofsky, L.A., Clark, B.E., Britt, D.T., 2000. The nature of M-Class asteroids from 3 μm observations. Icarus 145, 351–368.

Schläppi, B., Altwegg, K., Wurz, P., 2008. Asteroid exosphere: a simulation for the Rosetta flyby targets (2867) Steins and (21) Lutetia. Icarus 195, 674–685.

Schläppi, B., Altwegg, K., Balsiger, H., Hässig, M., Jäckel, A., Wurz, P., Fiethe, B., Rubin, M., Fuselier, S.A., Berthelier, J.J., De Keyser, J., Rème, H., Mall, U., 2010. Influence of spacecraft outgassing on the exploration of tenuous atmospheres with in situ mass spectrometry. Journal of Geophysical Research 115, A12313.

Schorghofer, H., 2008. The lifetime of ice on main belt asteroids. Journal of Geophysical Research 662, 697–705.

Snodgrass, C., Tubiana, C., Vincent, J.-B., Sierks, H., Hviid, S., Moissl, R., Boehnhardt, H., Barbieri, C., Koschny, D., Lamy, P., Rickman, H., Rodrigo, R., Carry, B., Lowry, S.C., Laird, R.J.M., Weissman, P.R., Fitzsimmons, A., Marchi, S., 2010. A collision in 2009 as the origin of the debris trail of asteroid P/2010 A2. Nature 467, 814–816.

Stern, S.A., Parker, J.Wm, Feldman, P.D., Weaver, H.A., Steffl, A., A'Hearn, M.F., Feaga, L., Birath, E., Graps, A., Bertaux, J.-L., Slater, D.C., Cunningham, N., Versteeg, M., Scherrer, J.R., 2011. Ultraviolet discoveries at asteroid (21) Lutetia by the Rosetta Alice ultraviolet spectrograph. Astronomical Journal 141, article 199. doi:10.1088/0004-6256/141/6/199.

Wirth, K.R., Küppers, M., Koschny, D., Dhiri, V., Vallat, C., Laureijs, R., Ho, T.-M., Schwehm, G., 2009. Scientific planning and commanding of the Rosetta payload. In: Schulz, R., Alexander, C., Boehnhardt, H., Glassmeier, K.-H. (Eds.), Rosetta, ESA's Mission to the Origin of the Solar System. Springer, pp. 151–166.

Wurz, P., Balough, A., Coffey, V., Dichter, B.K., Kasprzak, W.T., Lazarus, A.J., Lennartsson, W., McFadden, J.P., 2007. Calibration techniques. In: Wüest, M., Evans, D.S., Steiger, R. (Eds.), Calibration of Particle Instruments in Space Physics, ESA Communications, ISSI Scientific Report SR-007, pp. 117–276.